Photochemical aging of organic and inorganic ambient aerosol from the Potential Aerosol Mass (PAM) reactor experiment in East Asia

Eunha Kang[1,5], Meehye Lee[1]*, William H. Brune[2], Taehyoung Lee[3],

Joonyoung Ahn[4], Xiaona Shang[1]

[1]Department of Earth and Environmental Sciences, Korea University, Republic of Korea

[2]Department of Meteorology, Pennsylvania State University, USA

[3]Department of Environmental sciences, Hankuk University of Foreign Studies, Republic of Korea

[4]National Institute of Environmental Research, Republic of Korea

[5]Department of Urban and Environmental studies, Suwon Research Institute, Republic of Korea

Submitted to Atmospheric Chemistry & Physics

December 2016

* Corresponding author, meehye@korea.ac.kr

Abstract

We investigated the photochemical aging of ambient aerosols using a potential aerosol mass (PAM) reactor at Baengnyeong Island in the Yellow Sea during August 4–12, 2011. The size distributions and chemical compositions of the ambient and aged PAM aerosols were measured alternately every 6 min by Scanning Mobility Particle Sizer (SMPS) and High Resolution-Time of Flight-Aerosol Mass Spectrometer (HR-ToF-AMS), respectively. Inside the PAM reactor, O_3 and OH levels were equivalent to 4.6 days of integrated OH exposure at typical atmospheric conditions. Two types of air masses were distinguished on the basis of the chemical composition and the degree of aging: The air transported from China was more aged with higher sulfate concentration and O:C ratio and the air mass coming through the Korean Peninsula was less aged with more organics than sulfate and lower O:C ratio. In PAM reactor, sulfate was constantly formed, resulting in the increase of particle mass at 200–400 nm size range. Organics were responsible for an overall loss of mass in 100–200 nm particles. This loss was especially evident for the m/z 43 component representing less oxidized organics. Conversely, the m/z 44 component corresponding to further oxidized organics increased with a shift toward larger sizes during the organics-dominated episode. The oxidation of less oxidized organics was likely facilitated by gas-phase oxidation and partitioning for re-equilibrium between the gas and particle phases. Nitrate evaporated in the PAM reactor upon the addition of sulfate to the particles. These results suggest that the chemical composition of aerosols and their degree of photochemical aging particularly for organics are also crucial in determining aerosol mass concentrations. Because sulfate in the atmosphere was stable for about a week of the nominal lifetime of aerosols, SO_2 is an unquestionably primary precursor of secondary aerosol in northeast Asia. In comparison, the contribution of organics to secondary aerosols is more variable during transport in the atmosphere. Note that the integrated OH exposure of 4.6 days emphasized the sulfate contribution on aerosol in this study because further oxidation leads to the loss of OAs over a couple days of aging. Notably, an increase in low-volatility organics was associated with sulfate and evident at 200–400

nm, highlighting the potential role of secondary organic aerosol (SOA) in cloud condensation nuclei (CCN) formation.

1. Introduction

In East Asia, atmospheric aerosols are a cause of public concern because of the frequent occurrence of haze in mega cities and industrial areas and dust storms in deserts and extremely dry regions, and their transboundary transport (Takami et al., 2007; Wu et al., 2009; Kim et al., 2009; Ramana et al., 2010; Kang et al., 2013). These occurrences impact the regional air quality and climate (Li et al., 2011; Huang et al., 2014). Aerosol plumes are able to remain in the atmosphere for up to 10 days and can be transported across the Pacific Ocean. During transport, air masses become photochemically aged, leading to the generation of secondary aerosols and subsequent modification of the optical and microphysical properties of aerosols (Dunlea et al., 2009; Lim et al., 2014; Lee et al., 2015). This transformation process has been studied by collecting ambient air across the Pacific Ocean or by tracking the Asian plumes onboard aircrafts (Brock et al., 2004; Aggarwal and Kawamura, 2009; Dunlea et al., 2009; Peltier et al., 2008).

Secondary aerosols (SA) comprise inorganics such as sulfate and nitrate as well as organics. Of these, secondary organic aerosols (SOA) are of more interest because they are produced in the atmosphere from numerous organic species and are aged through complex mechanisms, during which their physicochemical properties such as volatility, hygroscopicity, and optical properties are altered. The absorption and scattering properties of aerosols in northeast Asia was reported to be intimately linked with their chemical composition (Lim et al., 2014). As aerosols are oxidized, the hygroscopicity of organic aerosols (OAs) increases, suggesting photochemically driven CCN activation of SOA (Massoli et al., 2010; Lambe et al., 2011; King et al., 2010; Morgan et al., 2010).

To understand SOA formation and aging processes, experiments have been conducted using environmental chambers (Kroll and Seinfeld, 2008; Hallquist et al., 2009).

In these large environmental chambers, atmospheric simulations are limited to the equivalent of only about a day, which is much shorter than the nominal lifetime of aerosols, which is about a week. In addition, ambient air masses are under influence of various emissions and mixing processes, which are not properly represented in these well-mixed and long-residence time chambers (Jimenez et al., 2009; Ng et al., 2010).

Thus, we introduced the potential aerosol mass (PAM) chamber, a continuous flow reactor under high levels of OH and O_3, which is applicable for both controlled lab studies and ambient air (Cubison et al., 2011; Kang et al., 2007, 2011b; Lambe et al., 2012; Massoli et al., 2010). The highly oxidizing conditions of the PAM reactor are suitable for examining SOA formation and oxidation processes for the equivalent of a week or more (Jimenez et al., 2009; George and Abbatt, 2010). In particular, the PAM reactor has less wall loss mainly due to much shorter residence time compared to conventional chambers. Thus, PAM reactor is able to reasonably simulate aging processes of SOA after formation (Kang et al., 2011a). In the first field deployment of PAM in northeast Asia, Kang et al. (2011a) reported PAM simulation results for different air masses and demonstrated that oxidation processes occurring in the natural atmosphere were plausibly integrated in the PAM reactor. Recently, PAM reactor has been used to examine secondary aerosol formation and evolution from ambient air masses (Hu et al., 2016; Ortega et al., 2016; Palm et al., 2016) and emission sources (Ortega et al., 2013; Link et al., 2017; Timonen et al., 2017). The wall losses of aerosols and condensable gases and photochemistry of the PAM reactors have been studied to quantitatively understand the experimental results of PAM reactor (Lamb et al., 2015; Palm et al., 2016; 2017; Peng et al., 2015; 2016). In this study, we deployed a PAM reactor at an island site in the Yellow Sea to investigate the photochemical aging processes of ambient aerosols such as secondary aerosol formation and evolution of pre-existing aerosol over the northeast Asia. Their size, mass, chemical, and transformation characteristics were thoroughly examined with a particular emphasis on SOA formation and transformation.

2. Experimental methods

Experiments were conducted at a measurement station on Baengnyeong Island in the Yellow Sea (37.967°N, 124.630°E, 100 m asl) from August 4 to August 12, 2011 (Fig. 1a). As the northernmost and westernmost part of South Korea, Baengnyeong Island is located 740 km west of Beijing and 211 km east of Seoul. The measurement station was established by the National Institute of Environmental Research (NIER) as a core background site of the National Monitoring Network to observe dust and pollution plume transported from China. In previous studies conducted at the same site, sulfate and organic aerosols were enhanced under the influence of pollution plumes transported from eastern China and the Korean Peninsula (Choi et al., 2016; Lee et al., 2015).

Ambient air sampled using a $PM_{1.0}$ cyclone and was pulled through a tubing (1 cm diameter) into the PAM reactor for 6 minutes, during which time the ambient aerosols were oxidized (hereafter referred to as "PAM aerosols"). For another 6 minutes, the sampled ambient air was directly pumped into the analytical instruments, bypassing the PAM reactor. The ambient and PAM aerosols were alternately measured every 6 minutes, thereby producing pseudo-simultaneous measurements.

The PAM reactor employed in this study is the same version as that described in Lambe et al. (2011), which was also used for laboratory studies of SOA aging (Lambe et al. 2012; 2015). The ambient air was introduced into the PAM reactor through an inlet plate and endcap and then rapidly dispersed before entering the reactor through a Silconert-coated (Silcotech, Inc.) stainless steel screen. For sampling, copper or stainless steel tubing was used to minimize the particle loss on the tubing walls. The residence time of air in the PAM reactor was 100 seconds based on flow rate and the volume of the reactor. During the experiment, the loss associated with PAM reactor and inlet was determined. The SO_2 loss through a cyclone and inlet plate was 11 ± 7 % and aerosol loss in the PAM reactor was about 12 %. The loss of aerosol and SO_2 gas was measured as difference in the concentration between ambient air and air pulled through PAM reactor with UV lights off.

The PAM reactor is equipped with long Hg lamps emitting 185 nm and 254 nm light (82-9304-03, BHK Inc.) in order to produce large amounts of OH and O_3, creating a highly oxidizing environment. The UV lamps were housed in Teflon sleeves being purged by nitrogen to prevent heat and O_3 from building up. The results of Ortega et al. (2016) using the PAM reactor same as that used in the present study, demonstrated that temperate was increased by about 2 ℃ inside the PAM reactor and its effect on evaporation of OA or nitrate was insignificant.

The OH exposure of PAM reactor was estimated to be 7 x 10^{11} molecules cm^{-3} s against sulfur dioxide decay that was conducted by Kang et al., 2011b. It is equivalent to an integrated OH concentration over 4.6 days at a typical noon-time concentration of 1.5 x 10^6 molecules cm^{-3} (Mao et al., 2010), which is lower by 25 % than was expected due to the external OH suppression. The OH suppression from VOCs and other OH-reactive gases were calculated using the chemistry model with 30 s^{-1} of external OH reactivity, representing rural areas (Feiner et al., 2016; Lee et al., 2008; Peng et al., 2016; Yoshino et al., 2006). In the present study, therefore, we examined how the air masses reaching Baegnyeong Island were further oxidized during the effective aging time of 4.6 days, which is consistent with transport time from China but slightly longer than the time of typical maximum SOA production from aging (Ortega et al., 2016) under OH diel-mean of 1.5 x 10^6 molecules cm^{-3}. The chemical composition of aerosol was measured by a high-resolution time-of-flight aerosol mass spectrometer (HR-ToF-AMS, hereafter referred to as "AMS") and their number concentration was determined in the mobility diameter range of 10.4–469.8 nm with a scanning mobility particle sizer (SMPS 3034, TSI) (Jayne et al., 2000; Jimenez et al., 2003; DeCarlo et al., 2006; Drewnick et al., 2006). The aerosol mass concentration was obtained from the volume concentration multiplied by a fixed particle density of 1.2 g cm^{-3}. Detailed descriptions of the HR-ToF-AMS and the sampling site can be found elsewhere (Lee et al., 2015). For concentrations measured by AMS, composition dependent collection efficiency was applied by adopting the result of Middlebrook et al. (2012). Ozone (O_3), elemental carbon (EC), and organic carbon (OC) were simultaneously

158 measured, along with meteorological parameters (Table 1). The HYSPLIT backward
159 trajectory model, which was developed by the National Oceanic and Atmospheric
160 Administration (NOAA), was used to examine the history of the sampled air masses (Wang
161 et al., 2009).
162
163 **3. Results**
164 **3.1. Measurement overview of ambient and PAM aerosols**
165
166 $PM_{1.0}$ aerosol mass concentrations varied from 0.5 to 38 μg m^{-3} for both the PAM
167 aerosols and the ambient aerosols (Figure 2a) during the entire experiment period. Choi et
168 al. (2016) reported the AMS measurements ($PM_{1.0}$) made at the same site during March-
169 April, 2012 and November-December, 2013, where $PM_{1.0}$ varied from the detection limit to
170 ~100 μg m^{-3}. These $PM_{1.0}$ concentrations were lower than those measured in Changdao
171 that is located in Bohai Sea (Hu et al., 2013; Choi et al., 2016; Lee et al., 2015). The PAM
172 aerosol masses were generally greater than the ambient aerosol masses, but not all the
173 time. The difference in mass concentrations between the PAM aerosols and the ambient
174 aerosols either a gain or loss of particle mass in the range of -3 ~ 7 μg m^{-3}, indicating that
175 photo-oxidation.
176 Particle mass distributions of the ambient and PAM aerosols were averaged for the
177 entire experiment and their difference is presented in Fig. 3. In the PAM chamber, nuclei-
178 mode particles were formed (average dN/dlogDp = 2 x 10^5 cm^{-3}) but their contribution to
179 the total aerosol mass was relatively insignificant due to their small sizes of less than 50
180 nm in diameter (Dp). In comparison, the mass of PAM aerosol was distinctively increased at
181 sizes larger than 200 nm. Particles between 50 and 200 nm in diameter were either lost or
182 produced in the PAM reactor, depending on the history of the air masses. The formation of
183 nuclei mode particles in PAM reactor were also observed in previous studies (Ortega et
184 al., 2016; Palm et al., 2016). The enhancement of accumulation mode particles was
185 dependent on the equivalent ages of PAM reactor and condensation sink (CS) by

preexisting aerosols. Major constituents including sulfate, organics, ammonium, and nitrate for both ambient and PAM aerosols are presented in Fig 3. Sulfate and ammonium concentrations in the PAM reactor were mostly higher or similar to those in the ambient air. In contrast, total organics and nitrate were mostly lower in the PAM aerosols than ambient aerosols.

The measurement results of PAM experiment include uncertainty associated with losses of condensable gases and aerosols in PAM reactor and sampling system. The condensable gases fate model for PAM reactors (Palm et al., 2016) predicts 57~66% and 62~81% of organic gases and sulfates to be condensed on the existing aerosols, respectively at 4.6 days of equivalent aging time. We used the same constants as those in Palm et al. (2016) for our PAM condition (residence time of 100 s and aging time of 4.6 days). The fraction of low-volatility gases that were not condensed in the PAM reactor was higher for organic-dominated case (33%) than sulfate-dominated case (27%) because of greater CS in latter than former. Previous studies showed that the SOA formation from VOCs including Semi/Intermediate Volatile Compounds (S/IVOCs) could be enhanced up to a few times greater than SOAs from VOCs only (Hayes et al., 2015; Palm et al., 2016). In our experiment, air masses that were transported from the Korean Peninsula or from east China for at least 1 day were sampled in the PAM reactor, thus it is likely that S/IVOCs were already partitioned into the aerosol phase, if existed and the loss of S/IVOCs or their contribution to SOA formation would be much less significant than was reported in previous studies. Nonetheless, S/IVOCs could be lost to the reactor inlet plate as well as reactor wall due to their low saturation vapor pressures, leading to the underestimation of their contribution to SOA formation in the PAM reactor of this study.

3.2. Organics- and sulfate-dominated episodes

Throughout the experiment, ambient aerosols were highly enhanced during two separate periods (shaded in Fig. 2a), with distinct differences in chemical composition

between the two. While the ambient air was enriched in organics during the first episode (August 6, 11 AM to August 7, 9 AM), sulfate was dominant in the second episode (August 9, 1 AM to August 9, 6 PM). During the two episodes, the levels of gaseous precursors including NOx, SO_2, and CO were higher than in the remaining periods (Fig. 4). However, the ratios of both SO_2/NOx and OC/EC were higher for the first case than the second case. It was opposite for O_3/CO ratios. These two cases were distinguished by the air masses backward trajectories (Fig. 1b). Higher concentrations of organics than sulfate during the first episode resulted from air that had passed through the Korean Peninsula. The sulfate-dominated air in the second episode had been transported from Southeast China. In addition, the air mass trajectories imply that sulfate-dominated aerosols lingered over the Yellow Sea and were aged more than the organic-dominated aerosols.

In addition, the aerosol masses differed in terms of size distributions between the two episodes (Fig. 5). The mass difference between the ambient and PAM aerosols (gain and loss) was greater in all size ranges for the organic-dominant episode than the sulfate-dominant episode. In the PAM reactor, the mass of particles smaller than 50 nm and larger than 200 nm increased, but it decreased in the size range of 100–200 nm. The particles masses of separate size range are summarized for ambient and PAM processed aerosols in Table 1. For the two cases, aerosol masses increased at nuclei (10-50 nm) and condensation (200-500 nm) mode in PAM reactor. At size between 50 and 200 nm, however, the mass of PAM-processed aerosol was not evidently increased during sulfate-dominated episode and even decreased during organic-dominated episode. The measurement results of size-separated chemical compositions provide detailed information on transformation processes in the PAM reactor. In general, sulfate increased but total organics and nitrate were reduced in the PAM reactor compared to the ambient aerosols (Fig. 6). The contribution of ammonium ions to the total mass was also greatest when aerosols were enriched in sulfate. The organic m/z 43 and m/z 44 components exhibited different behavior in the PAM reactor between the two episodes (Fig. 5). While m/z 43 decreased in the PAM reactor in both episodes, m/z 44 only increased during the sulfate-

dominant episode.

Therefore, the following discussion is focused on these two distinct aerosols episodes, for which the size-separated chemical compositions were thoroughly examined and compared in order to elaborate on the formation of secondary aerosols and the evolution of ambient aerosols upon photo-oxidation in the PAM reactor.

4. Discussion

4.1. Formation of nuclei-mode particles

In the current study, the formation of nuclei-mode particles (Dp <50 nm) was always observed in the PAM reactor. SO_2 is primarily responsible for the formation of new nuclei mode particles. In previous field studies, increases in the amounts of PAM aerosols were dependent on the ambient SO_2 concentrations (Kang et al., 2013). Palm et al. (2016) also observed the nuclei mode particles formed, competing for the role of condensation sink (CS) with preexisting accumulation mode particles. For the two episodes in this study, the number concentrations of nuclei-mode particles differed by less than an order of magnitude and SO_2 concentrations were similar. Chemical compositions are not available for nuclei-mode particles due to an AMS cut-off size of 50 nm in the present study. VOC concentrations for ambient air were not determined, either. In the previous laboratory experiment, Kang et al. (2011) examined the transient peaks of OA mass concentration at nuclei mode and smaller stable peaks at larger size range under high OH exposure. These transient peaks were supposed to be related to the non-linear oscillatory nucleation and growth of OA, which was referred by McGraw and Saunders (1984). An initial burst of particles followed by the oscillatory mode with a lower particle number density was explained by the competition between the rapid formation of nuclei mode clusters and the condensation onto new particle surfaces of condensable species.

4.2. Formation and evolution of organic aerosols

The SMPS mass size distributions highlight the size range of 100~200 nm, where PAM aerosol was reduced in mass only for organic-dominated episode (Fig. 5). Mohr et al. (2012) observed that the ambient Semi-Volatile Oxygenated Organic Aerosols (SV-OOAs) and Low-Volatile Oxygenated Organic Aerosols (LV-OOAs) were mostly found in the range of 100–200 nm and greater than 200 nm, respectively. In addition, the concentration of organic m/z 43 was higher in SV-OOAs than LV-OOAs. In the present study, the contribution of m/z 43 to total organics was greater in organics-dominated than sulfate-dominated episode. So was the loss of organics in PAM reactor. Volatility of organics with m/z 43 and 44 were previously described in Ng et al., (2011). These results suggest that there were less oxidized OAs (e.g., SV-OOAs) in the organics-dominated than the sulfate-dominated episode. The ratios of O:C were lower for organic-dominated aerosols than those of sulfate-dominated aerosols (Fig. 7). In conjunction with O:C ratio, the air mass trajectories (Fig. 1b) imply organics-dominated air masses were relatively less aged thereby, including more less oxidized OAs than those of the sulfate-dominated episode (Jimenez et al., 2009; Ng et al., 2011).

The AMS measurement results indicate that total organics and the organic m/z 43 component were consistently reduced in the PAM reactor. Possible loss mechanisms are the deposition of aerosols on the chamber wall (McMurry and Grosjean, 1985; La et al., 2016) and fragmentation reactions from further photo-oxidation to form products with higher vapor pressure (Lamb et al., 2012). As described in the section 3, the condensable organics loss by wall surface and by heterogeneous oxidation were calculated to be about 30~40%. For the entire experiment, the O:C ratios of PAM aerosols were greater than those of ambient aerosols, with O:C ratios corresponding to SV-OOAs and LV-OOAs (Jimenez et al., 2009). Thus, a chemical transformation from low O:C to high O:C is more likely to explain the organic mass loss.

Organics are known to be oxidized by OH undergoing functionalization and fragmentation. The pathway by which this occurs is determined by the oxidation state of the existing organic aerosols. Functionalization dominates in the early stage of oxidation,

298 which increases total organics and organic m/z 43, while fragmentation dominates in the
299 later stage of oxidation, reducing OA mass (Jimenez et al., 2009; Kroll et al., 2009; Chacon-
300 Madrid et al., 2010; Henry and Donahue, 2012; Lambe et al., 2012). For highly oxidized
301 OAs with O:C ratios greater than 0.4, fragmentation becomes especially dominant,
302 resulting in OA mass loss. In this study, the measured O:C ratios of the ambient aerosols
303 were greater than 0.4 for both episodes (Fig. 7), which indicates that the observed ambient
304 organic aerosols were aged enough to be fragmented. Figure 7 also shows PAM OAs have
305 higher O:C ratio and lower H:C ratio than ambient aerosols do and the Van Krevelen slope
306 (Δ(H:C)/ Δ(O:C)) of both episodes were about -0.6. In a laboratory PAM experiment, Lambe
307 et al. (2012) observed a similar tendency and explained that as SOA oxidized, the Van
308 Krevelen slope changed from minor fragmentation of carbonyl and acids/alcohol to major
309 fragmentation of acids. In addition, Hu et al. (2016) demonstrated that fragmentation
310 became an important pathway of OAs oxidation at OH exposure greater than 10^{11}
311 molecules cm^{-3} s. At OH exposure of 7 x 10^{11} molecules cm^{-3} s, they observed 20 % of OA
312 mass loss by volatilization followed by fragmentation of heterogeneous reaction products
313 on the particles. In the present study, the OH-induced OA mass loss in PAM reactor was
314 about 22 % and 37 % for organic-dominated and sulfate-dominated episode, respectively
315 at our OH exposure of 7 x 10^{11} molecules cm^{-3} s (Table 1).
316 In comparison, the organic m/z 44 mass increased in PAM aerosols for the
317 organics-dominated episode but not for the sulfate-dominant episode. In particular, the
318 increase in organic m/z 44 mass was associated with larger sizes than the organic m/z 43
319 mass loss (Fig. 6). As mentioned above, organic m/z 43 loss was significant for sizes less
320 than 200 nm in AMS diameter, but most of the increase in organic m/z 44 mass was
321 observed in the size greater than 200 nm. If particles grew in size by heterogeneous
322 oxidation of carbonyls to carboxylic acids on pre-existing particle surfaces, the mass
323 decrease in m/z 43 should also have been associated with an increase in the m/z 44 mass
324 by the addition of oxygen in the sulfate-dominated episode. During the sulfate-dominated
325 episode, however, there was no difference in the organic m/z 44 mass between the

ambient and PAM aerosols, implying that a gas-phase reaction in the photo-chemical oxidation of organic aerosols was involved. Thus, the mass increase of the m/z 44 component in PAM aerosols was considered in terms of gas-to-particle partitioning.

Upon being aged, OAs are not only formed from precursor gaseous phases but also evaporated by partitioning between gas and aerosol phases. The evaporated OAs possibly undergo chemical oxidation, being partitioned into aerosol phase again. Therefore, SOAs can form from the oxidation of evaporated primary OAs as well as VOCs and Intermediate VOCs (Donahue et al., 2009). The organic-dominated episode of this study was characterized by higher organic concentrations and higher OC/EC ratios than the sulfate-dominated episode, which implies the availability of primary OAs and relatively less loss by aging or greater SOA formation, compared to photo-chemically inert EC.

The oxidation of organics in the atmosphere can occur both in the gas phase and through heterogeneous reactions. The gas-phase reaction is tens of times faster than the heterogeneous reaction, being limited by diffusion to the particle surface (Lambe et al., 2012). In our experiment, it was not feasible to distinguish gas-phase oxidation of semi-volatile organics in equilibrium with the particle phase from heterogeneous oxidation of organics on the particle surface. Nonetheless, the main result of this study demonstrates that a distinct loss in m/z 43 was accompanied by little change in m/z 44, which supports the possibility that gas-phase oxidation was involved in SOA formation. The distributions of m/z 43-like compounds such as carbonyl groups with a semi-volatile nature in gaseous and particulate phases are controlled by the partitioning equilibrium between the two phases. In contrast, m/z 44-like compounds such as organic acid groups with low volatility tend to preferentially remain in the particle phase (Ng et al., 2011). It is, therefore, quite likely to occur in PAM reactor that the gas-phase concentration of m/z 43-like compounds was decreased by further oxidation, leading to evaporation of organic m/z 43 in particle phase to be re-equilibrated with the decreased concentration in gas phase. On the other hand, m/z 44-like compounds were sufficiently less volatile that they underwent little evaporation to the gas phase. During the ~100 s of the residence time in the PAM reactor,

the gas-phase reactions would be more efficient than relatively slower heterogeneous oxidation (Lambe et al., 2012). It was also found in a previous study that much less OA mass loss occurred for highly oxidized OAs with low volatility than for less oxidized OAs due to heterogeneous oxidation (Kessler et al., 2012). In addition to the loss of less oxidized organics (m/z 43), the AMS measurements indicated that highly oxidized OAs (m/z 44) were produced in the PAM reactor. In particular, the m/z 44 peak was found to occur in the same size range as that of sulfate. These results suggest that SOAs formed by gas-phase oxidation and subsequent condensation on the surface of existing sulfate particles. Indeed, robust evidence for this can be found in detailed laboratory studies of SOA formation on acidic seed particles (Jang et al., 2002; Jang et al., 2006; Kang et al., 2007)

In the present study, the overall mass spectra of organics indicate significant loss of less oxidized OAs (e.g., m/z 41, 42, 43, …) in the PAM reactor for both episodes. In addition, CO^+ and COO^+ groups increased and decreased in the PAM aerosols for the organic-dominant and sulfate-dominant episodes, respectively (Fig. 5). Therefore, the discussion on single mass of organic m/z 43 and m/z 44 will also be valid for the entire organic classes.

4.3. Formation and evolution of inorganic aerosols

In the PAM aerosols, sulfate concentrations were always greater than or similar to those of the ambient aerosols for the entire experiment period. This indicates a significant contribution of sulfate to secondary aerosols in the PAM reactor, in which sulfuric acid was produced through photo-oxidation of SO_2 under high OH exposure and then nucleated or was deposited on pre-existing particles (Kang et al., 2007). For the two selected cases especially, sulfate mass was noticeably increased in condensation mode where the condensation of gas on particle surfaces would be favored, particularly under highly oxidative conditions. Although nuclei-mode particles increased in number to a great extent, their mass contribution was insignificant at the ambient level of gaseous precursors. In this

study, the variation in ammonium concentrations was similar to that of sulfate (Fig. 2b). In addition, the equivalent ratios of sulfate and nitrate to ammonium indicated that the ambient particles were mostly acidic

In the organic-dominated episode, the increase of the PAM aerosol mass in particles larger than 200 nm resulted from the formation of sulfate and organic m/z 44 as described earlier (Figs. 5, 6), in which sulfate exhibited a broad peak in 200–500 nm particles, as in ambient air. In comparison, the sulfate increase shifted toward smaller sizes in the 200–400 nm range during the sulfate-dominant episode, leading to a sharp peak at 200 nm. Unlike the organic-dominated episode, the loss of organic m/z 43 was not accompanied by an increase in organic m/z 44 during the sulfate-dominated episode. The loss of organic m/z 43 was observed in smaller size than the increase in organic m/z 44 was observed. These features resulted in the difference in overall mass distributions between the two episodes shown in Fig. 5.

For organic dominated episode, the aerosol mass was decreased at 100-200 nm in PAM reactor, of which particles seemed to grow in size into the condensation mode by the addition of sulfuric acid formed from the oxidation of SO_2. In figure 6, m/z 44 of PAM aerosol was enhanced in the condensation mode (AMS size >200nm) where the sulfate of PAM aerosol was enhanced. It suggests that further oxidized OAs were formed together with sulfate at condensation mode in the PAM reactor. This then implies that photo-oxidation efficiently activates organic particles to become cloud condensation-mode particles under SO_2-sufficient conditions.

In addition, an increase in sulfate mass was noticeable between 200–400 nm. A major inorganic constituent, nitrate was lost in the PAM reactor during both episodes, with an ambient nitrate concentration that was comparable to the levels of sulfate and organics (Fig. 2b). The nitrate loss is rather explicit in the PAM reactor because of efficient conversion of SO_2 to sulfate, causing the aerosols to become acidic and causing particulate nitrate (HNO_3(p)) to evaporate. A plausible source of HNO_3(p) in the PAM reactor is the deposition of gaseous HNO_3(g) or heterogeneous reaction of NO_2 on the

particle surfaces (Underwood et al., 2001),even though the latter is not clearly understood. If a particle is acidic in the presence of sulfuric acids, nitrate easily evaporates back to the gas phase. As stated in section 2, the loss of nitrate by temperature-induced evaporation would be insignificant.

In organic-dominated episode, the balance of ammonium with sulfate and nitrate [(sulfate+nitrate)(μN)]/[ammonium(μN)] was 1.34 in ambient aerosol, which was reduced to 1.22 in PAM aerosol with enhanced sulfate and ammonium but with nitrate being lost. In sulfate-dominated episode, the ammonium balance remained unchanged in PAM aerosol due to an equivalent loss of nitrate over the condensation mode with its mode being shifted toward larger size. These results illustrate the role of sulfate in determining chemical compositions and mass loadings of aerosols in northeast Asia.

4.4. Atmospheric implications

The ambient OAs in the present study were moderately to well aged, as indicated by their O:C ratios greater than 0.4. They were chemically and physically transformed in the PAM reactor, resulting in increased O:C ratios and decreased OA mass concentrations by photochemical oxidation and fragmentation processes. Although the oxidant levels of OH and O_3 in the PAM reactor far exceeded the ambient levels, the H:C and O:C ratios of the ambient and PAM OAs were in close agreement with those observed in the atmosphere (Ng et al., 2011) (Fig 7). These results provide good evidence for the ability of the PAM reactor to accelerate oxidation processes in ambient air under high O_3 and OH conditions and to represent atmospheric aging of approximately 5 days without physical removal processes such as dry/wet deposition. It further confirms that the PAM reactor is applicable for field studies to observe aging processes of various types of precursors and aerosols including emission sources and long-range transported air masses.

The O:C ratios of OAs from this study were plotted against aging time and

compared with those observed in East Asia (Fig. 8), where the O:C ratios were found to increase with transport time across the Pacific Ocean (Takegawa et al., 2006; Takami et al., 2007; Dunlea et al., 2009). The O:C ratios of the bulk OAs depend on the concentrations of organic constituents because the saturation vapor pressure varies with the molecular weight of the organics (Donahue et al., 2006). Thus, the O:C ratios from different studies are not directly comparable if their OAs concentrations vary over a wide range. In Figure 8, OA concentrations ranged up to 10 μg m^3 and thus a comparison among different sets of measurements is suitable. In the real atmosphere, the fate and evolution of secondary aerosols could be affected by scavenging of oxidized OAs and inorganic aerosols on the cloud droplets by aqueous aerosol surface reaction (Dunlea et al., 2009), nucleation of new particles due to the entrainment of free tropospheric air (Song et al., 2010), or dry deposition on the dust particles (Dunlea at al., 2009). It is noteworthy that the increase in O:C ratios with photochemical aging was slightly higher in our results than in those of previous studies, which is possibly due to the omission of these scavenging processes in PAM reactor .

The results of this study imply that SO_2 plays a key role in increasing secondary aerosol concentrations in East Asia because the lifetime of SO_2 is longer than those of VOCs and because sulfate is relatively stable in the particle phase once formed, contrary to nitrate and organics. While SOA formation is more important near sources or in fresh air masses, OAs oxidation occurs continuously during the transport of air masses. The formation yield of sulfate from SO_2 is greater than that of organic aerosols during 3~4 days of aging in the Asian pollution plume because of fast depletion of SOA precursors (Dunlea et al., 2009), which is consistent to our results. In particular, this study indicates that relatively less aged OAs were in equilibrium with the gas phase, through which oxidation of less oxidized OAs was carried out, leading to increased OA mass in the CCN size range (200–400 nm). The increased O:C ratios rendered particles more hygroscopic, thereby facilitating their activation as CCNs (Massoli et al., 2010). Thus, climate effect of OA aging should be considered along with deceases in OA mass loading when they are

transported across long distances.

5. Conclusions

A PAM reactor was used to analyze ambient air at Baengnyeong Island in the northern part of the Yellow Sea during August 4–12, 2011. The chemical compositions and number concentrations of ambient and PAM aerosols were alternately determined with ToF-AMS and SMPS, respectively. The integrated OH exposure was equivalent to 4.6 days of atmospheric photo-oxidation. The results of the present study demonstrate that the high levels of OH and O_3 in the PAM reactor can expedite slow atmospheric reactions and that chemical aging processes of the natural atmosphere are plausibly represented.

During the experiment, two periods of noticeably enhanced aerosol concentrations with different chemical compositions and degrees of air mass aging were observed. While organic concentrations were highest during August 6–7 and sulfate was more elevated on August 9, the ratio of O:C was higher for the latter than the former. In addition, the size-dependent mass distributions of major constituents were clearly distinguished between the two episodes, which were used to understand the photochemical and volatile properties of the aerosols.

In the PAM reactor, sulfate formed in condensation mode in particle sizes between 200 and 400 nm and presumably in nucleation mode for particles smaller than 50 nm, which suggests that SO_2 was not limited in the study region for generating secondary aerosols, even during summer. In contrast, nitrate was lost in particles of all size ranges due to evaporation by the addition of sulfate. The total mass of organics was reduced in particles between 100 and 400 nm, where the loss in the m/z 43 component was evident for both episodes. In contrast, the more oxidized organic m/z 44 component was produced at larger sizes of 200–400 nm only during the organic-dominated episode. These results suggest partitioning of less oxidized OAs into a gas-phase that was in equilibrium with the particle phases. As the concentration of m/z 43 and total organics decreased

upon oxidation, less oxidized OAs were likely evaporated away from the particle phase in the process of re-equilibration.

As the air mass aged, the loss was apparent for photochemically and physically unstable component such as organics and nitrate, whereas sulfate was stable in the aerosol phase. Therefore, organics and nitrate are likely to be relatively more important in near-source regions while sulfate is probably dominant in areas far from the source. Note that caution needs to be exerted when interpreting the results of the present study, considering that only one OH exposure was used in the PAM reactor, and that maximum organic SOA mass may not have been observed. The results highlight the importance of chemical composition and oxidation processes in determining the aerosol-forming potential of an air mass. Although organic mass concentrations decreased with photochemical aging, OAs were transformed from less oxidized OAs to further oxidized OAs, as demonstrated by an increase in the organic m/z 44 component at sizes of 200–400 nm where sulfate was consistently increased. In conjunction with the increased O:C ratio of organics, this underscores the potential of organics to act as cloud condensation nuclei under SO_2-sufficient conditions.

510 Table 1. Meteorological parameters and measurement summary for organic-dominated
511 and sulfate-dominated episodes.

	Organic-dominated	**Sulfate-dominated**		
	Aug. 6, 11 AM~ Aug. 7, 9 AM	Aug. 9, 1 AM~ Aug. 9, 2 PM*		
Meteorological parameters				
Temp(℃)	26 ± 0.8	20 ± 0.6		
Relative humidity (%)	84 ± 7.7	96 ± 0.2		
Wind speed (m/s)	5 ± 1.6	8 ± 1.7		
Wind direction	easterly	southwesterly		
Weather mark	Cloudy	Fog		
Gaseous species				
SO_2 (ppbv)	3.1 ± 0.3	3.4 ± 0.2		
NO_2 (ppbv)	2.4 ± 0.8	0.9 ± 0.3		
CO (ppmv)	0.2 ± 0.0	0.4 ± 0.1		
O_3 (ppbv)	46 ± 22	54 ± 8		
Aerosol species[#]				
	Ambient	**PAM**	**Ambient**	**PAM**
Mass[&]	14.04±4.49	16.31±5.14	25.00±6.41	27.48 ± 7.32
10~50nm	0.03±0.03	0.66±0.30	0.01±0.01	0.24±0.10
50~200nm	5.55±2.33	4.73±1.99	7.78±2.01	7.83±2.09
200~500nm	8.45±2.27	10.92±3.15	17.21±5.49	19.41±6.65
Sulfate	2.95 ± 1.31	4.19 ± 1.81	11.45 ± 4.65	12.37 ± 4.68
Nitrate	1.16 ± 0.85	0.47 ± 0.21	1.56 ± 1.01	0.38 ± 0.18
Ammonium	1.03 ± 0.62	1.38 ± 0.63	3.44 ± 1.36	3.44 ± 1.37
Organics	10.59± 3.71	7.33 ± 2.54	5.34 ± 1.85	3.36 ± 0.95
m/z 43	0.66 ± 0.04	0.29 ±0.01	0.24 ± 0.02	0.09 ± 0.02
m/z 44	1.47 ± 0.08	1.76 ± 0.01	0.93 ± 0.06	0.86 ± 0.05

512 * Data from 9 AM to 12 AM, August 9 were excluded because of rain.

513 # Units are μg cm^{-3}.

514 [&] Aerosol mass concentrations were obtained from SMPS measurements with an aerosol
515 density of 1.2 μg cm^{-3} and sulfate, nitrate, ammonium and organics were from HR-ToF-
516 AMS measurements.

517

Figure Captions

Figure 1. (a) The location of the measurement site on Baengnyeong Island, the northernmost island in South Korea. The red circle indicates the measurement station location. (b) 72-hour backward trajectory for the two episodes. Green represents the organics-dominated episode during August 6, 11 AM to August 7, 9 AM, 2011, while red represents the sulfate-dominated episode during August 9, 1 AM to August 9, 2 PM, 2011.

Figure 2 (a) Aerosol mass concentrations from SMPS measurements for ambient and PAM aerosols. (b) Mass concentrations of major components measured by HR-ToF-AMS including organics, nitrate, sulfate, ammonium, chloride, and organic m/z 43 and m/z 44. Solid lines and lines with markers represent ambient aerosols and PAM aerosols, respectively. Shaded periods represent the organics-dominated episode (August 6, 11 AM to August, 7 9 AM) and the sulfate-dominated episode (August 9, 1 AM to August 9, 2 PM). The lowest mass concentration observed on August 8 was due to rain..

Figure 3. SMPS mass difference between PAM and ambient aerosols averaged for the entire sampling period.

Figure 4. Hourly measurements of SO_2, NOx, CO, O_3, and meteorological parameters for the entire sampling period.

Figure 5. (a) AMS mass spectra of organics and SMPS mass size distribution averaged for organics-dominated episode and (b) AMS mass spectra of organics and SMPS mass size distribution averaged for sulfate-dominated episode.

Figure 6. AMS p-ToF size distributions of PAM and ambient aerosol components averaged for each case.

Figure 7. Van Krevelen diagram for two episodes. Dashed lines represent the Van Krevelen

543 slopes, Δ(H:C)/ Δ(O:C) to show the direction of particular functional group
544 additions (Heald et al., 2010). Shaded gray areas represent the H:C and O:C ranges
545 observed in ambient OAs (Ng et al., 2011).
546 Figure 8. Comparison of O:C ratios in this study and other studies with respect to
547 photochemical age. The photochemical ages in our measurement were obtained
548 by the transport time calculated from a back trajectory analysis and
549 photochemical aging times in the PAM chamber. Other study data were obtained
550 from Takegawa et al. (2006), Takami et al. (2007), and Dunlea et al. (2009).

Figures

Figure 1(a)

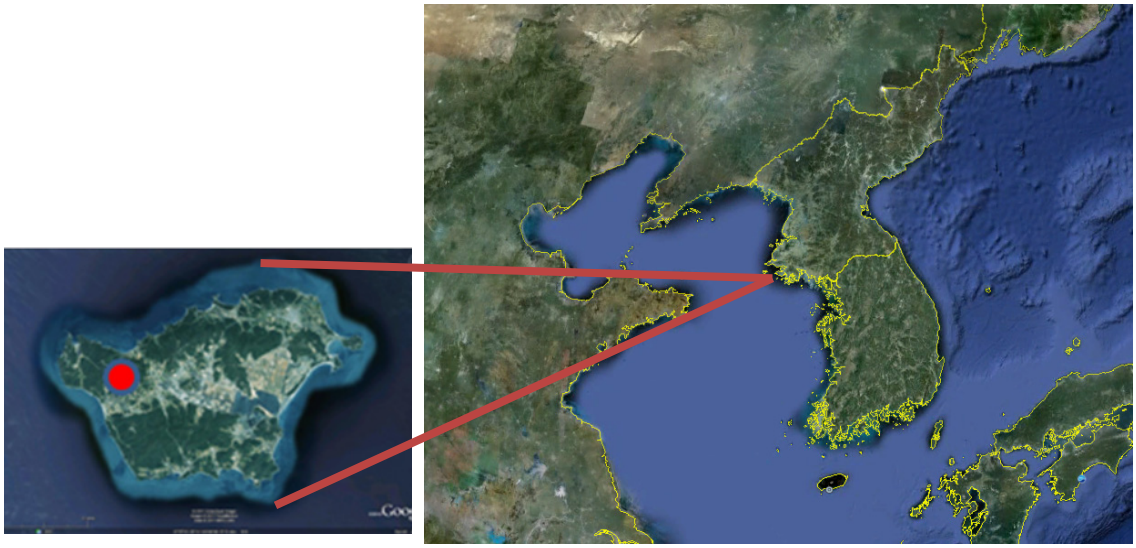

Figure 1(b)

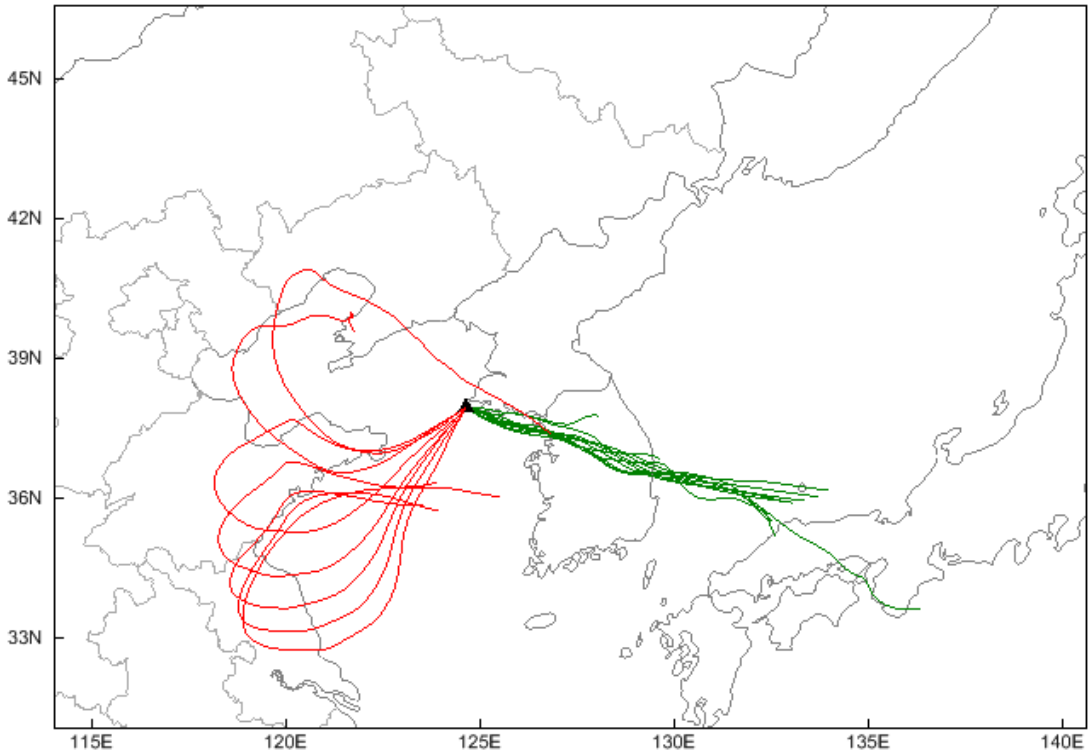

559 Figure 2(a)

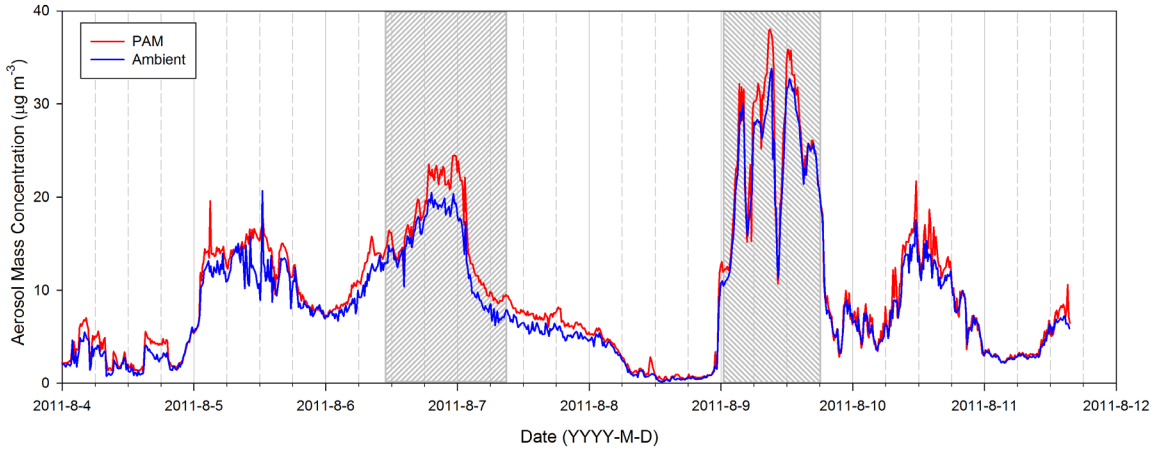

560

561

562 Figure 2(b)

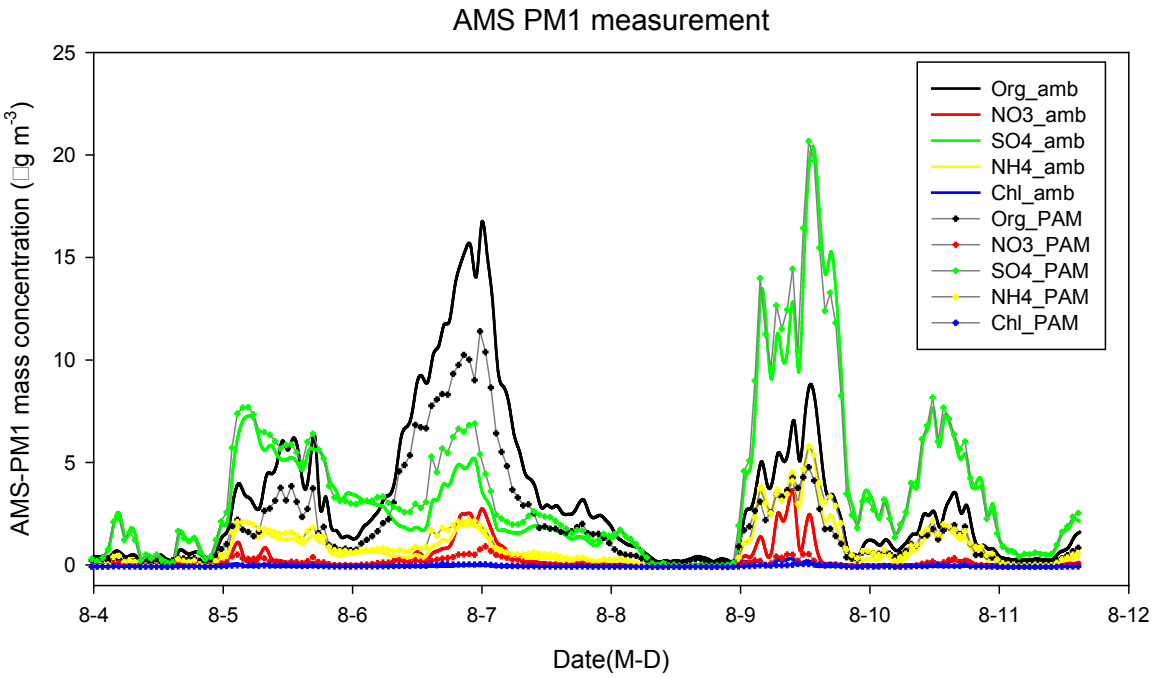

563

564

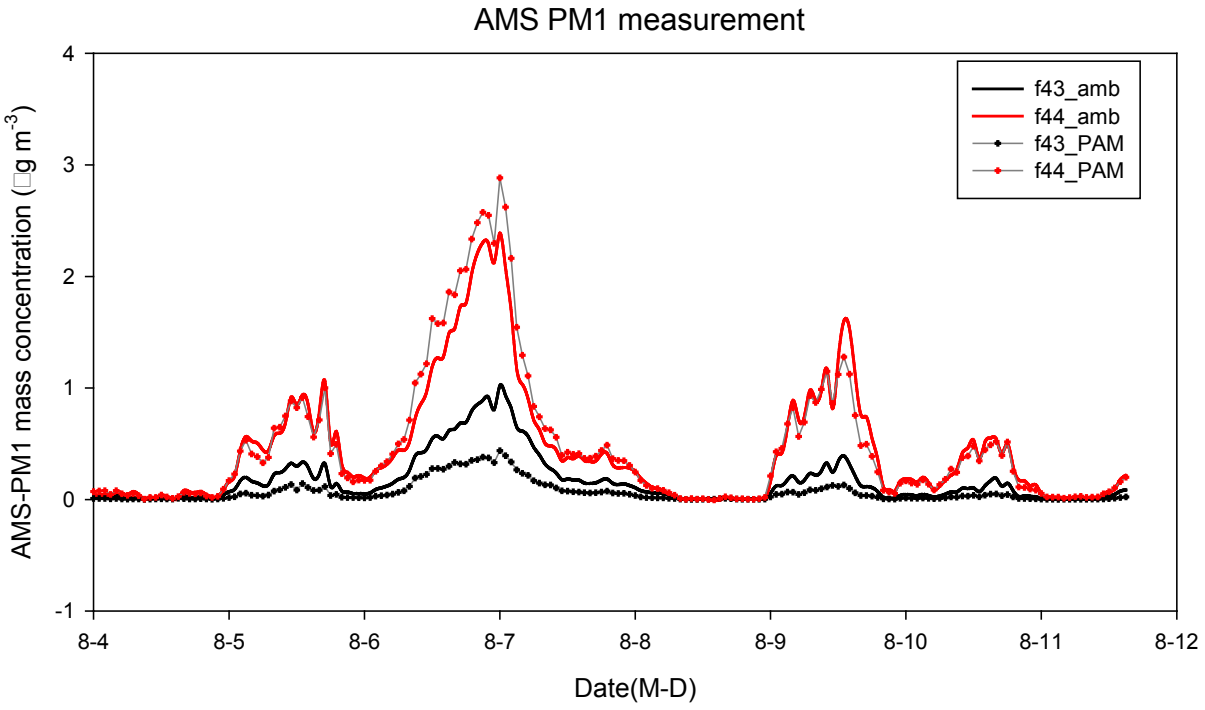
AMS PM1 measurement
AMS-PM1 mass concentration (□g m-3)
Date(M-D)
f43_amb
f44_amb
f43_PAM
f44_PAM
4
3
2
1
0
-1
8-4
8-5
8-6
8-7
8-8
8-9
8-10
8-11
8-12

565

566 Figure 3.

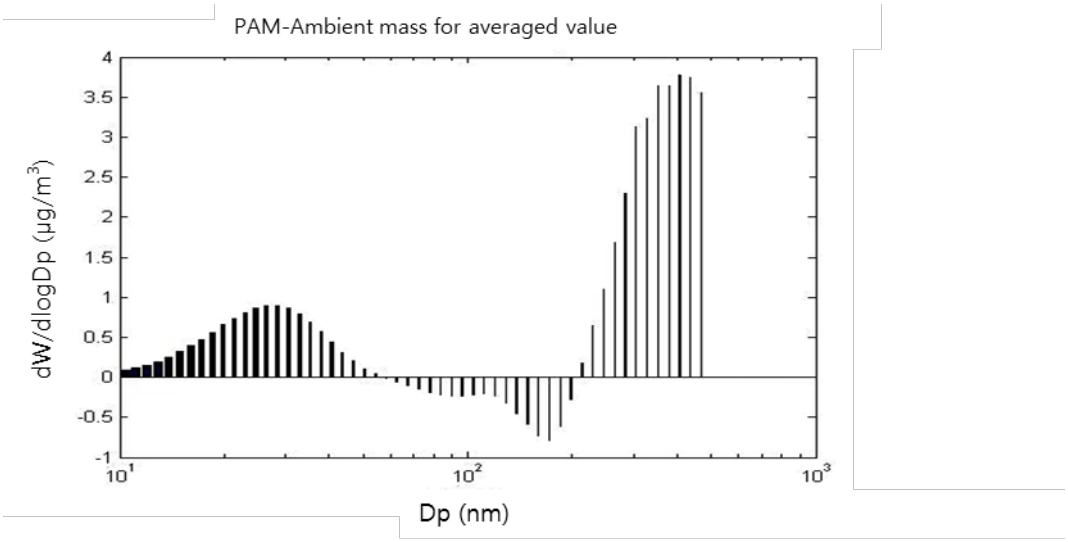

567

568 Figure 4.

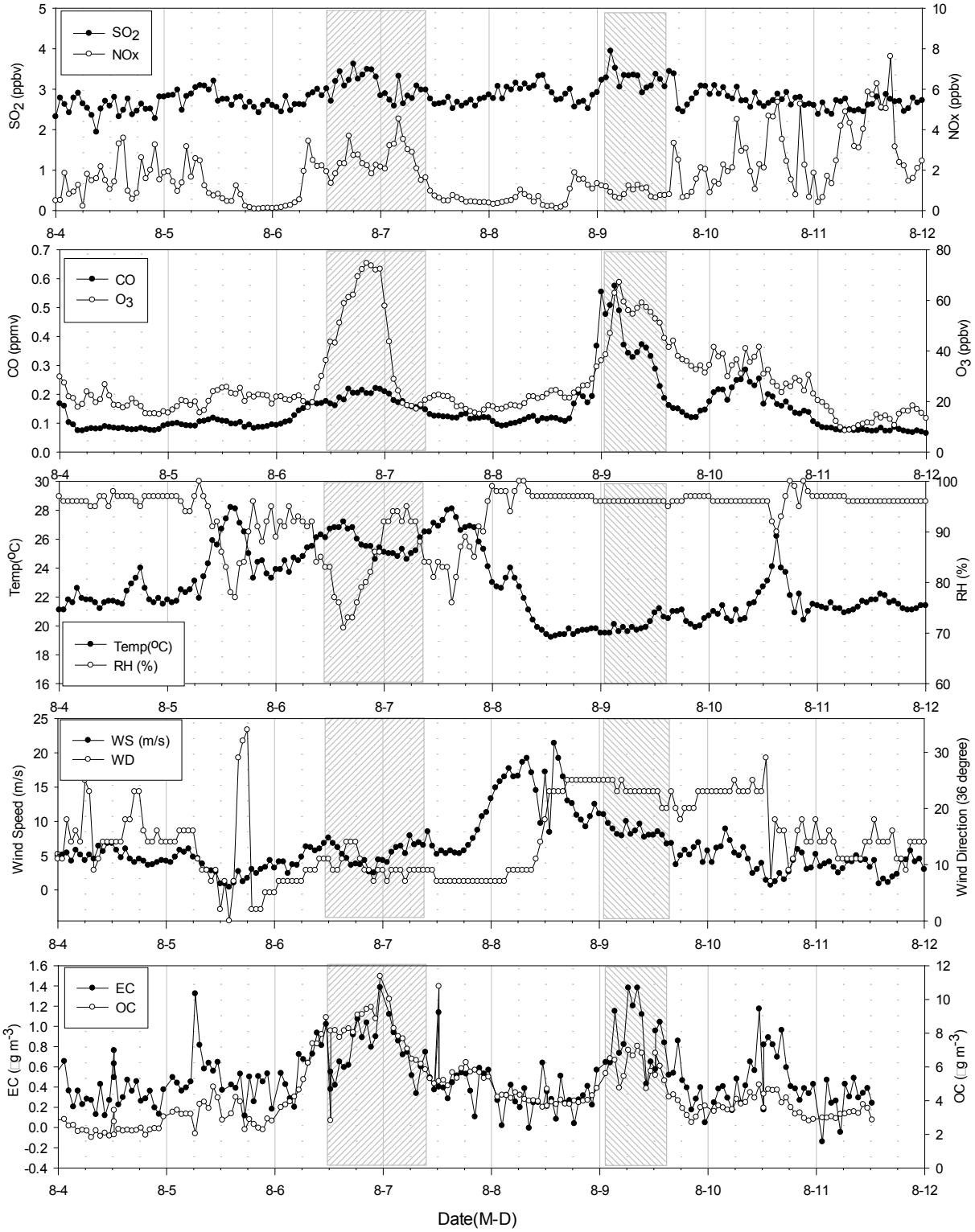

569

570

571 Figure 5(a)

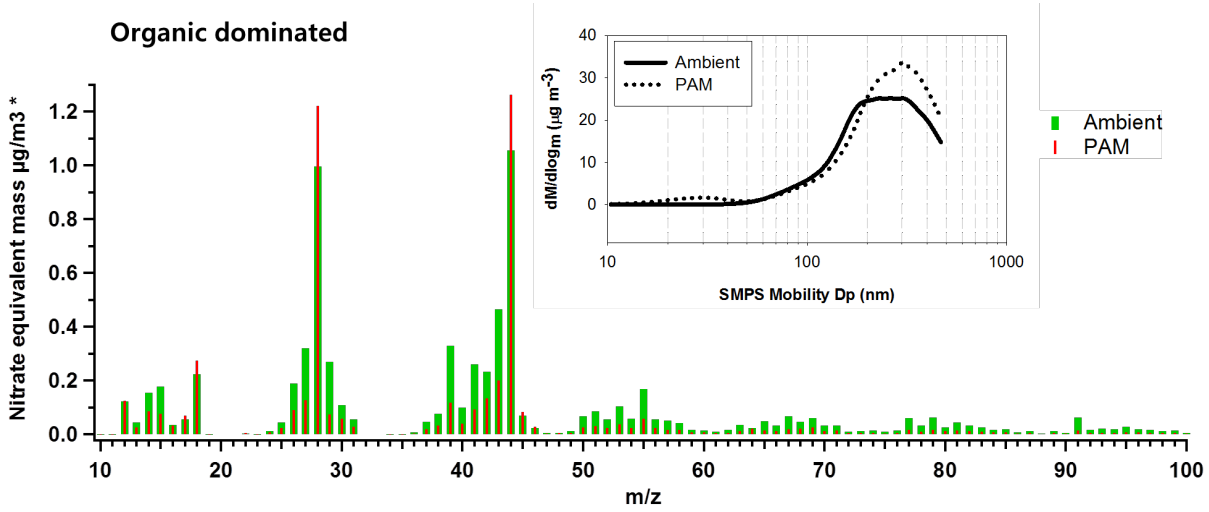

572

573

574 Figure 5(b)

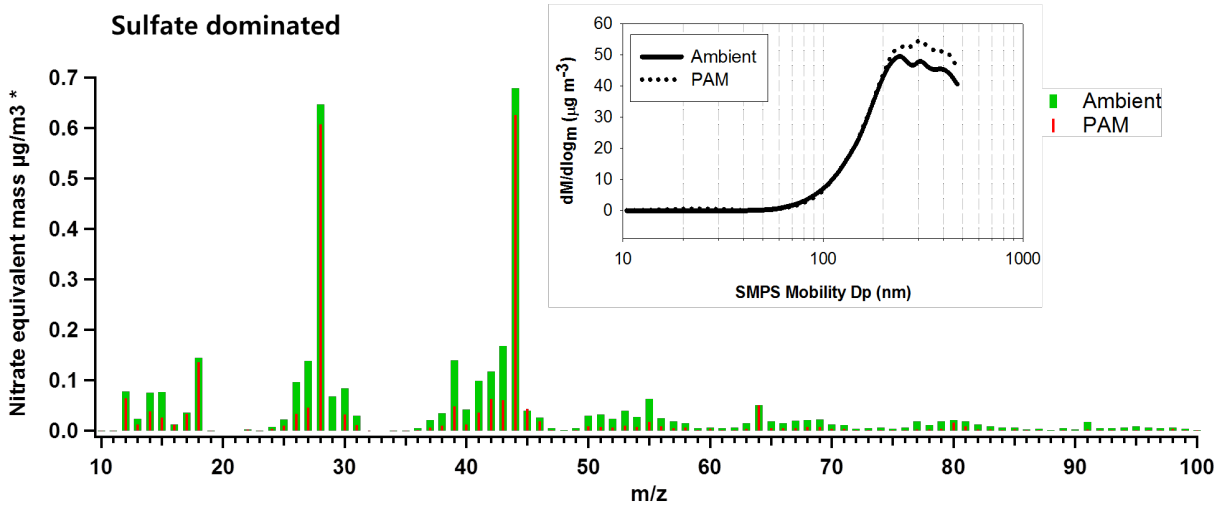

575

576

577

578 Figure 6.

579

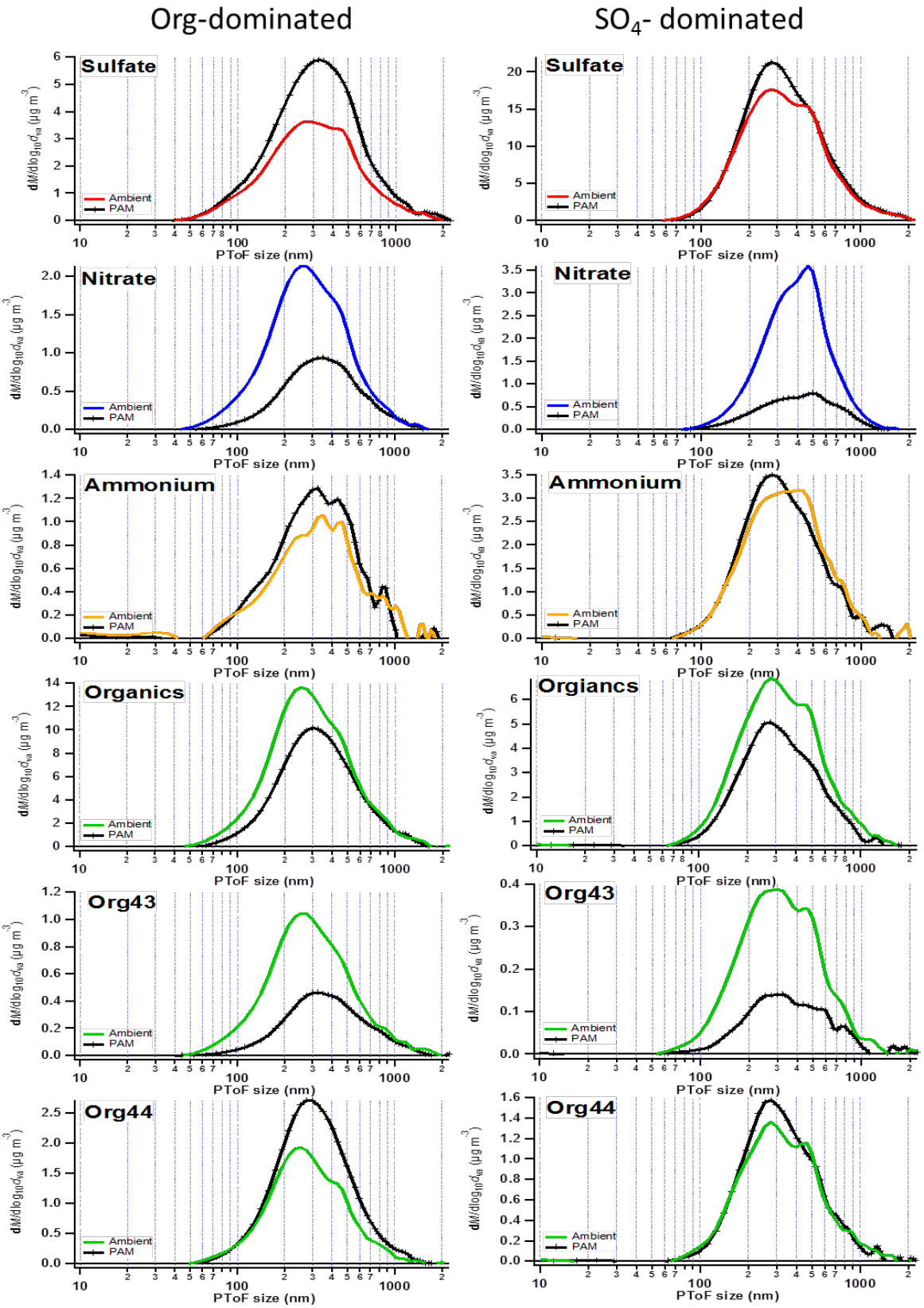

580 Figure 7.

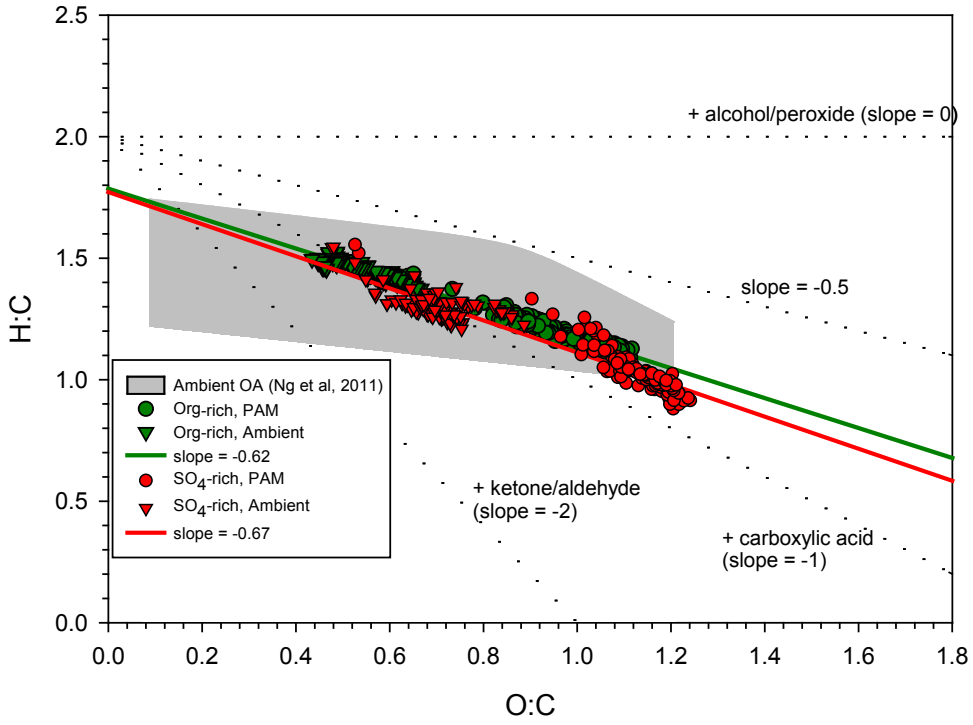

581

582

583 Figure 8.

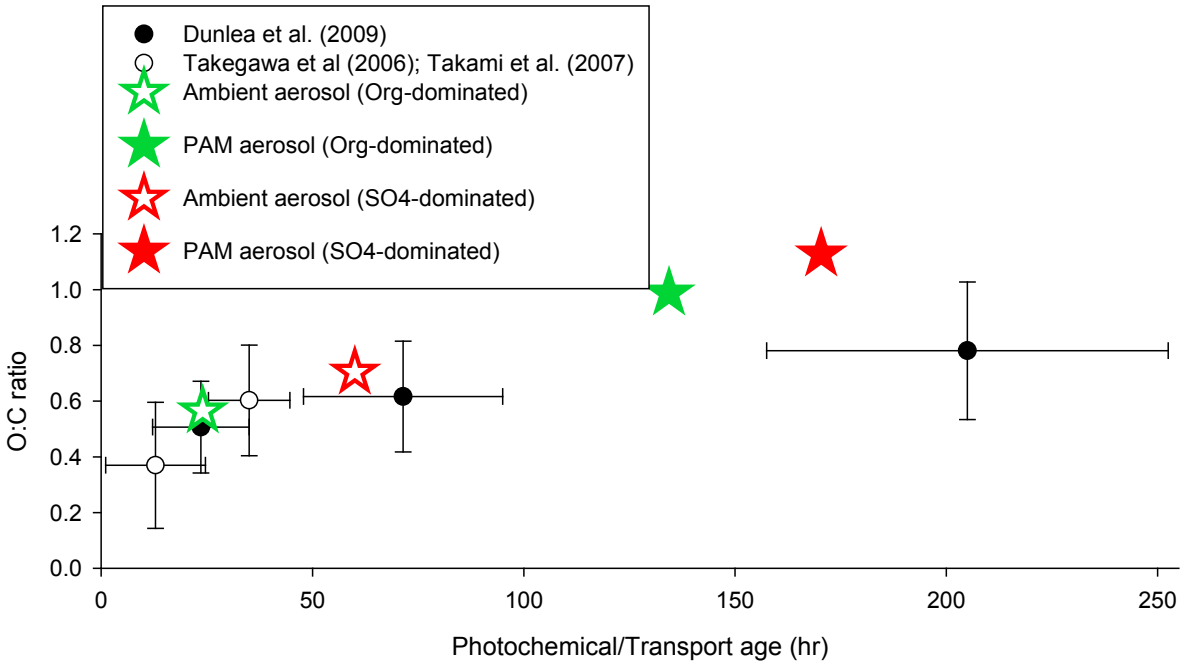

584

585

586 **References**

587

588 Aggarwal, S. G., and Kawamura, K.: Carbonaceous and inorganic composition in long-range
589 transported aerosols over northern Japan: Implication for aging of water-soluble organic
590 fraction, Atmospheric Environment, 43, 2532-2540, 2009.

591 Andreae, M. O., and Gelencser, A.: Black carbon or brown carbon? The nature of light-
592 absorbing carbonaceous aerosols, Atmos Chem Phys, 6, 3131-3148, 2006.

593 Bateman, A. P., Nizkorodov, S. A., Laskin, J., and Laskin, A.: Photolytic processing of
594 secondary organic aerosols dissolved in cloud droplets, Physical Chemistry Chemical
595 Physics, 13, 12199-12212, Doi 10.1039/C1cp20526a, 2011.

596 Brock, C. A., Hudson, P. K., Lovejoy, E. R., Sullivan, A., Nowak, J. B., Huey, L. G., Cooper, O.
597 R., Cziczo, D. J., de Gouw, J., Fehsenfeld, F. C., Holloway, J. S., Hubler, G., Lafleur, B. G.,
598 Murphy, D. M., Neuman, J. A., Nicks, D. K., Orsini, D. A., Parrish, D. D., Ryerson, T. B., Tanner,
599 D. J., Warneke, C., Weber, R. J., and Wilson, J. C.: Particle characteristics following cloud-
600 modified transport from Asia to North America, J Geophys Res-Atmos, 109, Artn D23s26
601 Doi 10.1029/2003jd004198, 2004.

602 Chacon-Madrid, H. J., Presto, A. A., and Donahue, N. M.: Functionalization vs.
603 fragmentation: n-aldehyde oxidation mechanisms and secondary organic aerosol formation,
604 Physical Chemistry Chemical Physics, 12, 13975-13982, Doi 10.1039/C0cp00200c, 2010.

605 Choi J., Kim, J., Lee, T., Choi, Y., Park, T., Oh, J., Park, J., Ahn, J., Jeon, H., Koo, Y., Kim, S.,
606 Hong, Y., and Hong, J.: A Study on Chemical Characteristics of Aerosol Composition at
607 West Inflow Regions in the Korean Peninsula I. Characteristics of PM Concentration and
608 Chemical Components, J.KOSAE., 32(5), 469-484, 2016

609 Cubison, M. J., Ortega, A. M., Hayes, P. L., Farmer, D. K., Day, D., Lechner, M. J., Brune, W.
610 H., Apel, E., Diskin, G. S., Fisher, J. A., Fuelberg, H. E., Hecobian, A., Knapp, D. J., Mikoviny, T.,
611 Riemer, D., Sachse, G. W., Sessions, W., Weber, R. J., Weinheimer, A. J., Wisthaler, A., and

612 Jimenez, J. L.: Effects of aging on organic aerosol from open biomass burning smoke in
613 aircraft and laboratory studies, Atmos Chem Phys, 11, 12049-12064, DOI 10.5194/acp-11-
614 12049-2011, 2011.

615 Donahue, N. M., Robinson, A. L., Stanier, C. O., and Pandis, S. N.: Coupled partitioning,
616 dilution, and chemical aging of semivolatile organics, Environ Sci Technol, 40, 2635-2643,
617 Doi 10.1021/Es052297c, 2006.

618 Dunlea, E. J., DeCarlo, P. F., Aiken, A. C., Kimmel, J. R., Peltier, R. E., Weber, R. J., Tomlinson,
619 J., Collins, D. R., Shinozuka, Y., McNaughton, C. S., Howell, S. G., Clarke, A. D., Emmons, L. K.,
620 Apel, E. C., Pfister, G. G., van Donkelaar, A., Martin, R. V., Millet, D. B., Heald, C. L., and
621 Jimenez, J. L.: Evolution of Asian aerosols during transpacific transport in INTEX-B, Atmos
622 Chem Phys, 9, 7257-7287, 2009.

623 Feiner, P., Brune, W., Miller, D., Zhang, L., Cohen, R., Romer, P., Goldstein, A., Keutsch, F.,
624 Skog, K., Wennberg, P., Nguyen, T., Teng, A., DeGouw, J., Koss, A., Wild, R., Brown, S.,
625 Guenther, A., Edgerton, E., Baumann, K., Fry, J.: Testing Atmospheric Oxidation in an
626 Alabama Forest. J. Atmos. Sci. 73(12), 4699-4710, 2016.

627 George, I. J., and Abbatt, J. P. D.: Chemical evolution of secondary organic aerosol from
628 OH-initiated heterogeneous oxidation, Atmos Chem Phys, 10, 5551-5563, DOI
629 10.5194/acp-10-5551-2010, 2010.

630 Gilardoni, S., Massoli, P., Giulianelli, L., Rinaldi, M., Paglione, M., Pollini, F., Lanconelli, C.,
631 Poluzzi, V., Carbone, S., Hilamo, R., Russell, L.M., Facchini, M.C., Fuzzi, S.: Fog scavenging of
632 organic and inorganic aerosol in the Po Valley, Atmos. Chem. Phys., 14, 6967-6981, 2014.

633 Hallquist, M., Wenger, J. C., Baltensperger, U., Rudich, Y., Simpson, D., Claeys, M., Dommen,
634 J., Donahue, N. M., George, C., Goldstein, A. H., Hamilton, J. F., Herrmann, H., Hoffmann, T.,
635 Iinuma, Y., Jang, M., Jenkin, M. E., Jimenez, J. L., Kiendler-Scharr, A., Maenhaut, W.,
636 McFiggans, G., Mentel, T. F., Monod, A., Prevot, A. S. H., Seinfeld, J. H., Surratt, J. D.,
637 Szmigielski, R., and Wildt, J.: The formation, properties and impact of secondary organic

638 aerosol: current and emerging issues, Atmos Chem Phys, 9, 5155-5236, 2009.

639 Hayes, P.L., Carlton, A.G., Baker, K.R., Ahmadov, R., Washenfelder, R.A., Alvarez, S.,
640 Rappenglück, Gilman, J.B., Kuster, W.C., de Gouw, J.A., Zotter, P., Prévôt, A.S.H., Szidat, S.,
641 Kleindienst, T.E., Offenber, J.H., Ma, P.K., Jimenez, J.L.: Modeling the formation and aging of
642 secondary organic aerosols in Los Angeles during CalNex 2010, Atmos. Chem. Phys., 15,
643 5773-5801, 2015.

644 Heald, C. L., Kroll, J. H., Jimenez, J. L., Docherty, K. S., DeCarlo, P. F., Aiken, A. C., Chen, Q.,
645 Martin, S. T., Farmer, D. K., and Artaxo, P.: A simplified description of the evolution of
646 organic aerosol composition in the atmosphere, Geophys Res Lett, 37, Artn L08803, Doi
647 10.1029/2010gl042737, 2010.

648 Henry, K. M., and Donahue, N. M.: Photochemical Aging of alpha-Pinene Secondary
649 Organic Aerosol: Effects of OH Radical Sources and Photolysis, J. Phys. Chem. A, 116, 5932-
650 5940, Doi 10.1021/Jp210288s, 2012.

651 Hu, W.W., Hu, M., Yuan, B., Jimenez, J.L., Tang, Q., Peng, J.F., Hu, W., Shao, M., Wang, M.,
652 Zeng, L.M., Wu, Y.S., Gong, Z.H., Huang, X.F., and He, L.Y.: Insights on organic aerosol aging
653 and the influence of coal combustion at a regional receptor site of central eastern China,
654 Atmos. Chem. Phys., 13, 10095-10112, 2013.

655 Hu, W., Palm, B.B., Day, D.A., Campuzano-Jost, P., Krechmer, J.E., Peng, Z., de Sá, S.S.,
656 Martin, S.T., Alexander, M.L., Baumann, K., Hacker, L., Kiendler-Scharr, A., Koss, A.R., de
657 Gouw, J.A., Goldstein, A.H., Seco, R., Sjostedt, S.J., Park, J.-H., Guenther, A.B., Kim, S.,
658 Canonaco, R., Prévôt, A.S.H., Brune, W.H., Jimenez, J.L.: Volatility and lifetime against OH
659 heterogeneous reaction of ambient isoprene-epoxydiols-derived secondary organic aerosol
660 (IEPOX-SOA), Atmos. Chem. Phys., 16, 11563-11580, 2016.

661 Huang, R.J., Zhang, Y., Bozzetti, C., Ho, K.F., Cao, J.J., Han, Y., Daellenbach, K.R., Slowik, J.G.,
662 Platt, S.M., Canonaco, F., Zotter, P., Wolf, R., Pieber, S.M., Bruns, E.A., Crippa, M., Ciarelli, G.,
663 Piazzalunga, A., Schwikowski, M., Abbaszade, G., Schnelle-Kreis, J., Zimmermann, R., An, Z.,

664 Szidat, S., Baltensperger, U., Haddad, I.E., and Prevot, A.S.H.: High secondary aerosol
665 contribution to particulate pollution during haze events in China, Nature, 514, 218-222,
666 2014.

667 Jang, M., Czoschke, N. M., Northcross, A. L., Cao, G., and Shaof, D.: SOA formation from
668 partitioning and heterogeneous reactions: Model study in the presence of inorganic
669 species, Environ Sci Technol, 40, 3013-3022, Doi 10.1021/Es0511220, 2006.

670 Jang, M. S., Czoschke, N. M., Lee, S., and Kamens, R. M.: Heterogeneous atmospheric
671 aerosol production by acid-catalyzed particle-phase reactions, Science, 298, 814-817, DOI
672 10.1126/science.1075798, 2002.

673 Jimenez, J. L., Canagaratna, M. R., Donahue, N. M., Prevot, A. S. H., Zhang, Q., Kroll, J. H.,
674 DeCarlo, P. F., Allan, J. D., Coe, H., Ng, N. L., Aiken, A. C., Docherty, K. S., Ulbrich, I. M.,
675 Grieshop, A. P., Robinson, A. L., Duplissy, J., Smith, J. D., Wilson, K. R., Lanz, V. A., Hueglin,
676 C., Sun, Y. L., Tian, J., Laaksonen, A., Raatikainen, T., Rautiainen, J., Vaattovaara, P., Ehn, M.,
677 Kulmala, M., Tomlinson, J. M., Collins, D. R., Cubison, M. J., Dunlea, E. J., Huffman, J. A.,
678 Onasch, T. B., Alfarra, M. R., Williams, P. I., Bower, K., Kondo, Y., Schneider, J., Drewnick, F.,
679 Borrmann, S., Weimer, S., Demerjian, K., Salcedo, D., Cottrell, L., Griffin, R., Takami, A.,
680 Miyoshi, T., Hatakeyama, S., Shimono, A., Sun, J. Y., Zhang, Y. M., Dzepina, K., Kimmel, J. R.,
681 Sueper, D., Jayne, J. T., Herndon, S. C., Trimborn, A. M., Williams, L. R., Wood, E. C.,
682 Middlebrook, A. M., Kolb, C. E., Baltensperger, U., and Worsnop, D. R.: Evolution of Organic
683 Aerosols in the Atmosphere, Science, 326, 1525-1529, DOI 10.1126/science.1180353, 2009.

684 Kang, E., Root, M. J., Toohey, D. W., and Brune, W. H.: Introducing the concept of Potential
685 Aerosol Mass (PAM), Atmos Chem Phys, 7, 5727-5744, 2007.

686 Kang, E., Brune, W. H., Kim, S., Yoon, S. C., Jung, M., and Lee, M.: A preliminary PAM
687 measurement of ambient air at Gosan, Jeju to study the secondary aerosol forming
688 potential, Journal of Korean Society for Atmospheric Environment, 27, 11, 2011a.

689 Kang, E., Toohey, D. W., and Brune, W. H.: Dependence of SOA oxidation on organic

690 aerosol mass concentration and OH exposure: experimental PAM chamber studies, Atmos
691 Chem Phys, 11, 1837-1852, DOI 10.5194/acp-11-1837-2011, 2011b.

692 Kang, E., Han, J., Lee, M., Lee, G., Kim, J.C.: Chemical characteristics of size-resolved
693 aerosols from Asian dust and haze episode in Seoul metropolitan city, Atmos. Res., 127,
694 34-46, 2013.

695 Kessler, S. H., Nah, T., Daumit, K. E., Smith, J. D., Leone, S. R., Kolb, C. E., Worsnop, D. R.,
696 Wilson, K. R., and Kroll, J. H.: OH-Initiated Heterogeneous Aging of Highly Oxidized
697 Organic Aerosol, J Phys Chem A, 116, 6358-6365, Doi 10.1021/Jp212131 m, 2012.

698 Kim, Y. J., Woo, J.-H., Ma, Y.-I., Kim, S., Nam, J. S., Sung, H., Choi, K.-C., Seo, J., Kim, J. S.,
699 Kang, C.-H., Lee, G., Ro, C.-U., Chang, D., and Sunwoo, Y.: Chemical characteristics of long-
700 range transport aerosol at background sites in Korea, Atmospheric Environment, 43, 5556-
701 5566, 2009.

702 King, S. M., Rosenoern, T., Shilling, J. E., Chen, Q., Wang, Z., Biskos, G., McKinney, K. A.,
703 Pöschl, U., and Martin, S. T.: Cloud droplet activation of mixed organic-sulfate particles
704 produced by the photooxidation of isoprene, Atmos. Chem. Phys., 10, 3953-3964,
705 10.5194/acp-10-3953-2010, 2010.

706 Kroll, J. H., and Seinfeld, J. H.: Chemistry of secondary organic aerosol: Formation and
707 evolution of low-volatility organics in the atmosphere, Atmospheric Environment, 42, 3593-
708 3624, DOI 10.1016/j.atmosenv.2008.01.003, 2008.

709 Kroll, J. H., Smith, J. D., Che, D. L., Kessler, S. H., Worsnop, D. R., and Wilson, K. R.:
710 Measurement of fragmentation and functionalization pathways in the heterogeneous
711 oxidation of oxidized organic aerosol, Physical Chemistry Chemical Physics, 11, 8005-8014,
712 Doi 10.1039/B905289e, 2009.

713 La, Y.S., Camredon, M., Ziemann, P.J., Valorso, R., Matsunaga, A., Lannuque, V., Lee-Taylor,
714 J., Hodzic, A., Madronich, S., and Aumont, B.: Impact of chamber wall loss of gaseous
715 organic compounds on secondary organic aerosol formation: explicit modeling of SOA

716 formation from alkane and alkene oxidation, Atmos. Chem. Phys., 16, 1417-1431,
717 2016.Lambe, A. T., Ahern, A. T., Williams, L. R., Slowik, J. G., Wong, J. P. S., Abbatt, J. P. D.,
718 Brune, W. H., Ng, N. L., Wright, J. P., Croasdale, D. R., Worsnop, D. R., Davidovits, P., and
719 Onasch, T. B.: Characterization of aerosol photooxidation flow reactors: heterogeneous
720 oxidation, secondary organic aerosol formation and cloud condensation nuclei activity
721 measurements, Atmos Meas Tech, 4, 445-461, DOI 10.5194/amt-4-445-2011, 2011.

722 Lambe, A. T., Onasch, T. B., Croasdale, D. R., Wright, J. P., Martin, A. T., Franklin, J. P.,
723 Massoli, P., Kroll, J. H., Canagaratna, M. R., Brune, W. H., Worsnop, D. R., and Davidovits, P.:
724 Transitions from Functionalization to Fragmentation Reactions of Laboratory Secondary
725 Organic Aerosol (SOA) Generated from the OH Oxidation of Alkane Precursors, Environ Sci
726 Technol, 46, 5430-5437, Doi 10.1021/Es300274t, 2012.

727 Lambe, A. T., Chhabra, P.S., Onasch,T.B., Brune, W.H., Hunter, J.F., Kroll, J.H., Cummings, M.J.,
728 Brogan, J.F., Parmar, Y., Worsnop, D.R., Kolb, C.E., and Davidovits, P.: Effect of oxidant
729 concentration, exposure time and seed particles on secondary organic aerosol chemical
730 composition and yield. Atmos. Chem. Phys.,15, 3063-3075, 2015.

731 Lee, M., Song, M., Moon, K. J., Han, J. S., Lee, G., and Kim, K. R.: Origins and chemical
732 characteristics of fine aerosols during the northeastern Asia regional experiment
733 (atmospheric brown cloud east Asia regional experiment 2005), J Geophys Res-Atmos, 112,
734 Artn D22s29 Doi 10.1029/2006jd008210, 2007.

735 Lee, T., Choi, J., Lee, G., Ahn, J., Park, J., Atwood, S.A., Schurman, M., Choi, Y., Chung, Y.,
736 Collett, Jr. J.L.: Characterization of Aerosol Composition, Concentrations, and Sources at
737 Baengnyeong Island, Korea using an Aerosol Mass Spectrometer, Atmospheric Environment
738 120, 297-306, 2015.

739 Li, Z., Li, C., Chen, H., Tsay, S.C., Holben, B., Huang, J., Li, B., Maring, H., Qian, Y., Shi, G., Xia,
740 X., Yin, Y., Zheng, Y., Zhuang, G.: East Asian studies of tropospheric aerosols and their
741 impact on regional climate (EAST-AIRC): An overview, J. Geophys. Re., 116, D00L34,
742 doi:10.1029/2010JD015257, 2011.

743 Lim, S., Lee, M., Kim, S.W., Yoon, S.C., Lee, G., and Lee, Y.J.: Absorption and scattering
744 properties of organic carbon versus sulfate dominant aerosols at Gosan climate
745 observatory in Northeast Asia, Atmos. Chem. Phys., 14, 7781-7793, 2014.

746 Link, M.F., Kim, J., Park, G., Lee, T., Park, T., Babar, Z.B., Sung, K., Kim, P., Kang, W., Kim, J.,
747 Choi, Y., Son, J., Lim, H.-J., Farmer, D.K.: Elevated production of NH_4NO_3 from the
748 photochemical processing of vehicle exhaust: Implications for air quality in the Seoul
749 Metropolitan Region, Atmos. Environ., 156, 95-101, 2017.

750 MaMurry, P.H. and Grosjean, D.: Gas and aerosol wall losses in Teflon film smog chambers,
751 Environ. Sci. Technol., 19(12), 1176-1182, 1985.

752 Mao, J., Ren, X., Chen, S., Brune, W.H., Chen, Z., Martinez, M., Harder, H., Lefer, B.,
753 Rappenglueck, B., Flynn, J., Leuchner, M.,: Atmospheric oxidation capacity in the summer of
754 Houston 2006: Comparison with summer measurements in other metropolitan studies,
755 Atmospheric Environment, 44, 4107–4115, 2010.

756 Massoli, P., Lambe, A. T., Ahern, A. T., Williams, L. R., Ehn, M., Mikkila, J., Canagaratna, M. R.,
757 Brune, W. H., Onasch, T. B., Jayne, J. T., Petaja, T., Kulmala, M., Laaksonen, A., Kolb, C. E.,
758 Davidovits, P., and Worsnop, D. R.: Relationship between aerosol oxidation level and
759 hygroscopic properties of laboratory generated secondary organic aerosol (SOA) particles,
760 Geophys. Res. Lett, 37, Artn L24801, Doi 10.1029/2010gl045258, 2010.

761 McGraw, R., Saunders, J.H.: A condensation feedback mechanism for oscillatory nucleation
762 and growth, Aerosol Science and Technology, 3(4), 367-380, 1984.

763 Middlebrook, A.M., R. Bahreini, J.L. Jimenez, and M.R. Canagaratna. Evaluation of
764 Composition-Dependent Collection Efficiencies for the Aerodyne Aerosol Mass
765 Spectrometer using Field Data. Aerosol Sci. Technol., 46, 258–271, 2012.Mohr, C., DeCarlo,
766 P. F., Heringa, M. F., Chirico, R., Slowik, J. G., Richter, R., Reche, C., Alastuey, A., Querol, X.,
767 Seco, R., Penuelas, J., Jimenez, J. L., Crippa, M., Zimmermann, R., Baltensperger, U., and
768 Prevot, A. S. H.: Identification and quantification of organic aerosol from cooking and other

769 sources in Barcelona using aerosol mass spectrometer data, Atmos Chem Phys, 12, 1649-
770 1665, DOI 10.5194/acp-12-1649-2012, 2012.

771 Morgan, W. T., Allan, J. D., Bower, K. N., Esselborn, M., Harris, B., Henzing, J. S., Highwood,
772 E. J., Kiendler-Scharr, A., McMeeking, G. R., Mensah, A. A., Northway, M. J., Osborne, S.,
773 Williams, P. I., Krejci, R., and Coe, H.: Enhancement of the aerosol direct radiative effect by
774 semi-volatile aerosol components: airborne measurements in North-Western Europe,
775 Atmos Chem Phys, 10, 8151-8171, DOI 10.5194/acp-10-8151-2010, 2010.

776 Ng, N. L., Canagaratna, M. R., Zhang, Q., Jimenez, J. L., Tian, J., Ulbrich, I. M., Kroll, J. H.,
777 Docherty, K. S., Chhabra, P. S., Bahreini, R., Murphy, S. M., Seinfeld, J. H., Hildebrandt, L.,
778 Donahue, N. M., DeCarlo, P. F., Lanz, V. A., Prevot, A. S. H., Dinar, E., Rudich, Y., and
779 Worsnop, D. R.: Organic aerosol components observed in Northern Hemispheric datasets
780 from Aerosol Mass Spectrometry, Atmos Chem Phys, 10, 4625-4641, DOI 10.5194/acp-10-
781 4625-2010, 2010.

782 Ng, N. L., Canagaratna, M. R., Jimenez, J. L., Chhabra, P. S., Seinfeld, J. H., and Worsnop, D.
783 R.: Changes in organic aerosol composition with aging inferred from aerosol mass spectra,
784 Atmos Chem Phys, 11, 6465-6474, DOI 10.5194/acp-11-6465-2011, 2011.

785 Ortega, A.M., Day, D.A., Cubison, M.J., Brune, W.H., Bon, D., de Gouw, J.A., Jimenez, J,L.:
786 Secondary organic aerosol formation and primary organic aerosol oxidation from biomass-
787 burning smoke in a flow reactor during FLAME-3, Atmos. Chem. Phys., 13, 11551-11571,
788 2013.

789 Ortega, A. M., Hayes, P. L., Peng, Z., Palm, B. B., Hu, W., Day, D. A., Li, R., Cubison, M. J.,
790 Brune, W. H., Graus, M., Warneke, C., Gilman, J. B., Kuster, W. C., de Gouw, J., Gutiérrez-
791 Montes, C., and Jimenez, J. L.: Real-time measurements of secondary organic aerosol
792 formation and aging from ambient air in an oxidation flow reactor in the Los Angeles area,
793 Atmos. Chem. Phys., 16, 7411-7433, doi:10.5194/acp-16-7411-2016, 2016.

794 Palm, B. B., Campuzano-Jost, P., Ortega, A. M., Day, D. A., Kaser, L., Jud, W., Karl, T., Hansel,

795 A., Hunter, J. F., Cross, E. S., Kroll, J. H., Peng, Z., Brune, W. H., and Jimenez, J. L.: In situ
796 secondary organic aerosol formation from ambient pine forest air using an oxidation flow
797 reactor, Atmos. Chem. Phys., 16, 2943-2970, doi:10.5194/acp-16-2943-2016, 2016.

798 Palm, B. B., Campuzano-Jost, P., Day, D. A., Ortega, A. M., Fry, J. L., Brown, S. S., Zarzana, K.
799 J., Dube, W., Wagner, N. L., Draper, D. C., Kaser, L., Jud, W., Karl, T., Hansel, A., Gutiérrez-
800 Montes, C., and Jimenez, J. L.: Secondary organic aerosol formation from in situ OH, O3,
801 and NO3 oxidation of ambient forest air in an oxidation flow reactor, Atmos. Chem. Phys.
802 Discuss., doi:10.5194/acp-2016-1080, 2017.

803 Peng, Z., Day, D. A., Stark, H., Li, R., Lee-Taylor, J., Palm, B. B., Brune, W. H., and Jimenez, J.
804 L.: HOx radical chemistry in oxidation flow reactors with low-pressure mercury lamps
805 systematically examined by modeling, Atmos. Meas. Tech., 8, 4863-4890, doi:10.5194/amt-
806 8-4863-2015, 2015.

807 Peng, Z., Day, D. A., Ortega, A. M., Palm, B. B., Hu, W., Stark, H., Li, R., Tsigaridis, K., Brune,
808 W. H., and Jimenez, J. L.: Non-OH chemistry in oxidation flow reactors for the study of
809 atmospheric chemistry systematically examined by modeling, Atmos. Chem. Phys., 16,
810 4283-4305, doi:10.5194/acp-16-4283-2016, 2016.

811 Peltier, R. E., Hecobian, A. H., Weber, R. J., Stohl, A., Atlas, E. L., Riemer, D. D., Blake, D. R.,
812 Apel, E., Campos, T., and Karl, T.: Investigating the sources and atmospheric processing of
813 fine particles from Asia and the Northwestern United States measured during INTEX B,
814 Atmos. Chem. Phys., 8, 1835-1853, 2008.

815 Ramana, M. V., Ramanathan, V., Feng, Y., Yoon, S. C., Kim, S. W., Carmichael, G. R., and
816 Schauer, J. J.: Warming influenced by the ratio of black carbon to sulfate and the black-
817 carbon source, Nat Geosci, 3, 542-545, Doi 10.1038/Ngeo918, 2010.

818 Richter, A., Burrows, J. P., Nuss, H., Granier, C., and Niemeier, U.: Increase in tropospheric
819 nitrogen dioxide over China observed from space, Nature, 437, 129-132,
820 10.1038/nature04092, 2005.

821 Song, M., Lee, M., Kim, J.H., Yum, S.S., Lee, G., Kim, K-R.: New particle formation and
822 growth in relation to vertical mixing and chemical species during ABC-EAREX2005, Atmos.
823 Res., 97, 359-370, 2010.

824 Sun, Y. L., Zhang, Q., Schwab, J. J., Chen, W. N., Bae, M. S., Lin, Y. C., Hung, H. M., and
825 Demerjian, K. L.: A case study of aerosol processing and evolution in summer in New York
826 City, Atmos Chem Phys, 11, 12737-12750, DOI 10.5194/acp-11-12737-2011, 2011.

827 Takami, A., Miyoshi, T., Shimono, A., Kaneyasu, N., Kato, S., Kajii, Y., and Hatakeyama, S.:
828 Transport of anthropogenic aerosols from Asia and subsequent chemical transformation, J
829 Geophys Res-Atmos, 112, Artn D22s31, Doi 10.1029/2006jd008120, 2007.

830 Takegawa, N., Miyakawa, T., Kondo, Y., Jimenez, J. L., Zhang, Q., Worsnop, D. R., and
831 Fukuda, M.: Seasonal and diurnal variations of submicron organic aerosol in Tokyo
832 observed using the Aerodyne aerosol mass spectrometer, J Geophys Res-Atmos, 111, Artn
833 D11206, Doi 10.1029/2005jd006515, 2006.

834 Timonene, H., Karjalainen, P., Asukko, E., Saarikoski, S., Aakko-Saksa, P., Simonen, P.,
835 Murtonen, T., Maso, M.D., Kuuluvainen, H., Bloss, M., Ahlberg, E., Svenningsson, B., Pagels,
836 J., Brune, W.H., Keskinen, J., Worsnop, D.R., Hillamo, R., Rönkkö, T.: Influence of fuel ethanol
837 content on primary emissions and secondary aerosol formation potential for a modern
838 flex-fuel gasoline vehicle, Atmos. Chem. Phys., 17, 5311-5329, 2017.

839 Underwood, G.M., Song, C.H., Phadnis, M., Carmichael, G.R., Grassian, V.H.: Heterogeneous
840 reactions of NO_2 and HNO_3 on oxides and mineral dust: A combined laboratory and
841 modeling study, J. Geophys. Res., 106(D16), 18055-18066, 2001.

842 Wang, Y. Q., Zhang, X. Y., and Draxler, R. R.,: TrajStat: GIS-based software that uses various
843 trajectory statistical analysis methods to identify potential sources from long-term air
844 pollution measurement data, Environ. Modell. Softw. 24, 938-939, 2009.

845 Wu, Z. J., Cheng, Y. F., Hu, M., Wehner, B., Sugimoto, N., and Wiedensohler, A.: Dust events
846 in Beijing, China (2004–2006): comparison of ground-based measurements with columnar

847 integrated observations, Atmos. Chem. Phys., 9, 6915-6932, 10.5194/acp-9-6915-2009,
848 2009.

849 Zhang, J., Wang, Y., Huang, X., Liu, Z., Ji, D., Sun, Y.: "Characterization of organic aerosols in
850 Beijing using an aerodyne high-resolution aerosol mass spectrometer", Adv. Atmos. Sci.,
851 32(6), 877-888, 2015.

852

853

854 **Acknowledgement**

855

856 This research was supported by Basic Science Research Program through the National
857 Research Foundation of Korea (NRF) funded by the Ministry of Science, ICT & Future
858 Planning (2017012143). E. Kang specially thanks for the support from the Basic Science
859 Research Program through the National Research Foundation of Korea(NRF) funded by the
860 Ministry of Education (NRF-2011-355-c00174).